https://doi.org/10.5194/essd-2026-738
Preprint. Discussion started: 16 November 2026
© Author(s) 2026. CC BY 4.0 License.



Open Access Earth System Science Data Discussions

Global time series of annual nitrogen stable isotope maps derived from Landsat: 30m, 1984-2023

Jinyan Yang[1,2]*, Jamie Vleeshouwer[2], Haiyang Zhang[3]**, Yiqing Guo[4], Xiaotao Lü[5], Xiaoguang Wang[8], Yunting Fang[6,7], Peter B. Reich[9,10], Xingguo Han[11,12], Karel Mokany[2], Robert Bridgart[13], Senani Karunaratne[1], Tim R. McVicar[2]

Affiliations:
[1] CSIRO Agriculture & Food, Canberra, ACT, 2601, Australia

[2] CSIRO Environment, Canberra, ACT, 2601, Australia

[3] College of Life Sciences, Hebei University, Baoding, China

[4] CSIRO Data61, Canberra, ACT, 2601, Australia

[5] Erguna Forest-Steppe Ecotone Research Station, CAS Key Laboratory of Forest Ecology and Management, Institute of Applied Ecology, Chinese Academy of Sciences, Shenyang China

[6] CAS Key Laboratory of Forest Ecology and Management, Institute of Applied Ecology, Chinese Academy of Sciences, Shenyang, China

[7] Qingyuan Forest CERN, CAS Key Laboratory of Forest Ecology and Management, Institute of Applied Ecology, Chinese Academy of Sciences, Shenyang, China

[8] College of Environment and Resources, Dalian Minzu University, Dalian, China

[9] Institute for Global Change Biology and School for Environment and Sustainability, University of Michigan, Ann Arbor, MI, USA

[10] Department of Forest Resources, University of Minnesota, St. Paul, MN, USA

[11] State Key Laboratory of Vegetation and Environmental Change, Institute of Botany, Chinese Academy of Sciences, Beijing, China

[12] University of Chinese Academy of Sciences, Beijing, China

[13] CSIRO Environment, Clayton, Vic, 3168, Australia

Correspondence to:
*Jinyan Yang (jinyan.yang@csiro.au)
** Haiyang Zhang (zhanghaiyang798@gmail.com)

Abstract. The lack of knowledge on how nitrogen cycles respond to environmental changes globally is a critical gap in assessing the sustainability of current terrestrial ecosystem services and projecting future carbon sink. The absence of spatiotemporal continuity in current nitrogen-cycle observations limits our understanding of how nitrogen cycles respond climate change. Plant nitrogen stable isotope ($\delta^{15}N$) serves as an integrator of nitrogen cycles, allowing quantification of how nitrogen cycles change. Existing on-ground data allow for estimation of $\delta^{15}N$ based on the established relationship between $\delta^{15}N$ and plant reflectance, providing the basis for large-scale long-term monitoring of $\delta^{15}N$ with satellite-based surface spectra.

Here we describe a novel method that calculates the annual $\delta^{15}N$ globally based on Landsat reflectance from 1984 to 2023 with planned updates for coming years using Google Earth Engine. The resulting spatio-temporal data include four channels: (i) mean $\delta^{15}N$ values; (ii) prediction uncertainty; (iii) the number of Landsat retrievals used; and (iv) a data quality assessment. We also demonstrate ways to access and visualise the maps and time series at various spatiotemporal scales with minimal requirements on programming skills and

https://doi.org/10.5194/essd-2026-738
Preprint. Discussion started: 16 November 2026
© Author(s) 2026. CC BY 4.0 License.



computational capacity. Finally, we show applications of the $\delta^{15}N$ maps for identifying drivers of $\delta^{15}N$ variation. The framework is open access on the cloud, providing all users easy access to nitrogen cycle monitoring. The dataset is available at DOI: https://doi.org/10.25919/zxvv-bj04 (Yang et al., 2026). A web-based application provides code-free access and visualisation to the dataset: https://tern-landscapes.earthengine.app/view/nitrogen-availability.

Key words: Nitrogen cycles, remote sensing, Landsat, ecosystem monitoring, global change, ^{15}N

1 Introduction

The terrestrial nitrogen cycle is strongly affected by anthropogenic environmental changes (Galloway et al., 2008; Mason et al., 2022). Rising atmospheric carbon dioxide concentration can stimulate plant growth and thus increase nitrogen demand (Hungate et al., 2003; Walker et al., 2021; Ruehr et al., 2023). On the other hand, increasing temperature and altered rainfall patterns changes soil microbial activities (Jansson and Hofmockel, 2022) and affects plant growth (Zhu et al., 2016). In addition, disturbance such as fire (Bowman et al., 2020), land use change (Jaureguiberry et al., 2022), and atmospheric nitrogen deposition (Tian et al., 2023) dramatically affect regional nitrogen cycles. A critical unresolved question in global change ecology is whether plants will have sufficient nitrogen to sustain growth under future environmental conditions (Luo et al., 2004; Reich et al., 2008).

Foliar nitrogen stable isotope ratio ($\delta^{15}N$) is increasingly used to investigate the impacts of environmental change on the terrestrial nitrogen cycle. Over the past century, ground-based observations suggest that foliar $\delta^{15}N$ has declined, often attributed to increased plant nitrogen demand under elevated CO_2 (BassiriRad et al., 2003; Garten et al., 2011; Polley et al., 2015; Kou et al., 2020). Consequently, researchers argue the observed global decline of $\delta^{15}N$ indicating that nitrogen is becoming more limiting for plant growth globally (BassiriRad et al., 2003; Craine et al., 2009; Craine et al., 2018; Kou et al., 2020; Mason et al.,2022, Tang et al., 2022). However, $\delta^{15}N$ is affected by multiple environmental drivers (Robinson et al., 2001; Craine, 2015). For example, anthropogenic nitrogen inputs into terrestrial ecosystems (Tian et al., 2022) could cause a similar decline of $\delta^{15}N$ (Hiltbrunner et al., 2019). Thus, it remains unclear whether CO_2 is the sole driver of the observed $\delta^{15}N$ change, and if not, what are the contributions of other environmental drivers to this pattern.

The confusion is rooted in the existing observations on foliar $\delta^{15}N$ that are spatially sparse and temporally discontinuous. Global and regional synthesis of foliar $\delta^{15}N$ provide data collected from fewer than 6,000 sites worldwide (Craine et al., 2018; Kou et al., 2020; Mason et al., 2022; Tang et al., 2022; Wang et al., 2022). More importantly, not all species/sites show consistent change over time (McLauchlan et al., 2010; Hietz et al., 2011;

https://doi.org/10.5194/essd-2026-738
Preprint. Discussion started: 16 November 2026
© Author(s) 2026. CC BY 4.0 License.



Open Access Earth System Science Data Discussions

Brookshire et al., 2020; Kou et al., 2020; Tang et al., 2022). Whether the differences among the studies are a result of sampling or an intrinsic heterogeneity among ecosystems and species remains unknown. Exploring the processes behind the change in $\delta^{15}N$ requires continuous large-scale observations that cover more ecosystems and species.

Leaf reflectance has been shown to capture foliar $\delta^{15}N$ at leaf scale (Serbin et al., 2014; Hellmann et al., 2015; Chen et al., 2022). At the canopy scale, this relationship can be maintained, but only after accounting for factors such as canopy structure and leaf angle (Wang et al., 2007). Radiative transfer models have been used to downscale canopy measurements to leaf reflectance (e.g., PROSAIL; Jacquemoud et al., 2009). However, their applications have been limited to site- and regional-scale studies due to high computational demand and challenges in parameterisation. Yang et al. (2025) developed an efficient method to map $\delta^{15}N$, using a random forest model and cross validation to account for the impacts of canopy structure. Unlike most other machine learning approaches, their model is trained only on Landsat spectra without incorporating environmental covariates. While their existing map achieves broad coverage, its spatial resolution remains coarse (~0.1 degree). Applying their approach to generate finer resolution spatiotemporal data and ensuring easy public access would benefit numerous future ecosystem monitoring and modelling studies.

Here we implemented the framework developed in Yang et al. (2025) within Google Earth Engine (GEE) to map foliar $\delta^{15}N$ globally at 30 m resolution using Landsat data. The resulting spatiotemporal data, along with the associated prediction uncertainties, are publicly available (https://doi.org/10.25919/zxvv-bj04). We also developed a web-based app to allow anyone with internet access to analyse, visualise, and download the data (https://tern-landscapes.earthengine.app/view/nitrogen-availability).

2 Methods

We moved the workflow developed by Yang et al. (2025) to GEE to generate $\delta^{15}N$ maps (Fig 1). We built a random forest model between on-ground $\delta^{15}N$ data and Landsat reflectance, which was then used for generating the $\delta^{15}N$ maps. The four key advancements over Yang et al. (2025) included: (i) higher spatial resolution; (ii) the addition of prediction uncertainty and quality control layers; (iii) coding-free data visualisation and download; and (iv) open access via cloud computing.

https://doi.org/10.5194/essd-2026-738
Preprint. Discussion started: 16 November 2026
© Author(s) 2026. CC BY 4.0 License.



Open Access Earth System Science Data Discussions

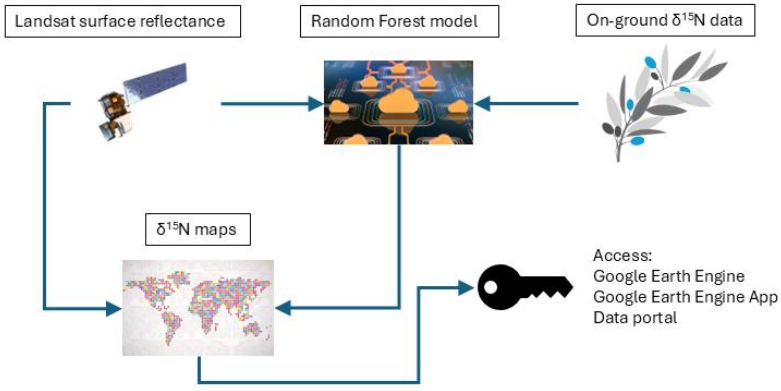


Figure 1. Conceptual workflow of the approach used to generate and distribute global maps of $\delta^{15}N$. Here we applied the method developed in Yang et al. (2025) on GEE and focused on improving accessibility and coverage.

2.1 Input datasets

The ground-based foliar $\delta^{15}N$ data were obtained from Yang et al. (2025) and split into training and testing datasets in the 70:30 ratio randomly. This resulted in 38,197 observations from 5,345 sites worldwide. We used Landsat Collection 2 Tier 1 calibrated Surface Reflectance from Landsat 5 and 8 on GEE (Gorelick et al. 2017). Since the Landsat 5 and 8 reflectance have been inter-calibrated, we did not apply harmonisation between products. The quality assessment channel (Bitmask for QA_PIXEL) of Landsat was used to remove pixels covered by cloud and cloud shadow. Water bodies were filtered by a digital elevation map (Jarvis et al., 2008). We calculated NDVI of each Landsat retrieval and removed data with NDVI < 0.2 to remove reflectance of areas with low vegetation cover and/or bare soil (Montandon and Small, 2008).

2.2 $\delta^{15}N$ mapping

2.2.1 Random forest model

We used the random forest model implemented in the SMILE package (Li, 2014), fitting ten models each with 50 trees in each model, resulting a total number of 500 trees. The independent variables comprised six Landsat bands (i.e., red, blue, green, near-infrared, short-wave infrared 1, short-wave infrared 2), while the dependent variable was ground-based foliar $\delta^{15}N$. For all ten models, the number of splits was set to two. Final $\delta^{15}N$ estimates were obtained by averaging predictions across the models, with the standard deviation among models

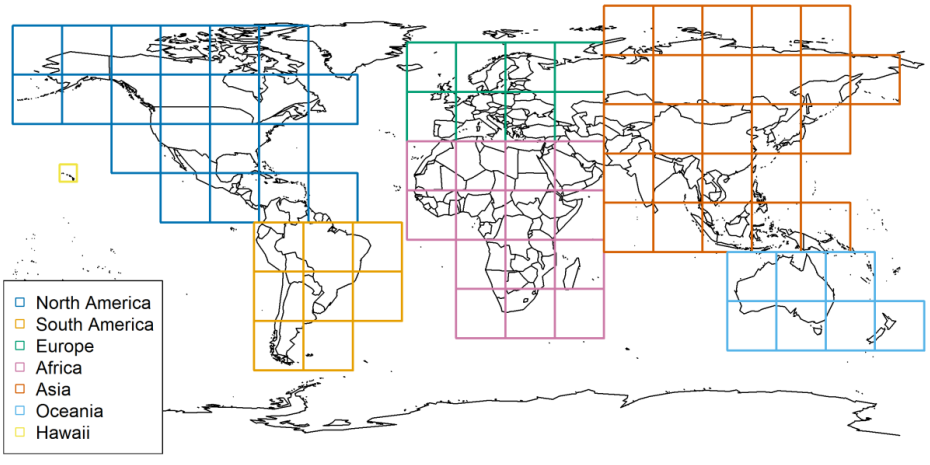
https://doi.org/10.5194/essd-2026-738
Preprint. Discussion started: 16 November 2026
© Author(s) 2026. CC BY 4.0 License.



representing prediction uncertainty. Independent evaluation achieving a normalised root mean square error of 0.15–0.20 across land cover types has been previously reported (Yang et al., 2025). The method has been evaluated by Yang et al. (2025) reporting a normalised root mean square error of 0.15–0.20 across land cover types.

2.2.3 Cloud computing

The global land surface (excluding Antarctica, Greenland and small island nations) was split into 85 tiles (Fig 2), each 20-degrees longitude by 20-degrees latitude. The processing was performed on a per-tile per-annum basis on GEE with all Landsat retrievals that passed the filtering used. One annual mean $\delta^{15}N$ is reported for each pixel. Processing time per tile varied greatly depending on the amount of land in each tile and the number of Landsat images acquired over each tile. For example, processing one year for a tile containing the Hawaiian Islands archipelago took about 20 mins, whereas a tile in the centre of CONUS (land only) required about 24 hours for the same period. Leveraging GEE's parallel processing capabilities (per tile), each annual dataset was generated in one day. Given 39 complete years (1984-2023, excluding 2012 due to data gap between Landsat products), the full global time-series required approximately four weeks to produce on GEE.



https://doi.org/10.5194/essd-2026-738
Preprint. Discussion started: 16 November 2026
© Author(s) 2026. CC BY 4.0 License.



Figure 2. Polygons of the regions used to generate tiles of $\delta^{15}N$. Note that the polygon boundaries were defined for computational purposes and do not necessarily correspond to the geographical boundaries of the continents or regions after which they are named.

2.2.4 Output data format, structure and spatiotemporal coverage

Each $\delta^{15}N$ image contained four bands: (i) the annual $\delta^{15}N$ (d15n_mean); (ii) the prediction uncertainty (d15n_stdDev) which was the standard deviation of all trees; (iii) the number of Landsat reflectance retrieval used to derive $\delta^{15}N$ (n_count); and (iv) the quality assessment (pixel_qa). The pixel_qa band used bit mask with 0 = good quality; 1 = water body mask; 2 = cloud/cloud shadow mask; 3 = NDVI mask. The current version excluded most of Greenland and most oceanic islands, except Hawaii, nonetheless, interested users could map the $\delta^{15}N$ of those regions with the provided code. All maps were projected in EPSG:4326.

2.3 Known limitations

The maps were not intended for croplands or areas with species that are selectively cultivated by humans, as the training and testing datasets contained no observations of those species/ecosystems. We provided examples to use land cover maps to filter out areas with high probability of presence of those ecosystems. However, this filtering did not account for actual species composition (e.g., a pixel could be highly modified pasture but labelled as grassland). The filter also only reflected land cover changes occurring after 2001. Users are advised to use a land use land cover filter that is customised for their needs.

The training and testing datasets are spatially biased, resulting in a limited coverage of plants from many regions in the world. The datasets are also temporally discontinuous, resulting in the fitting and testing being vulnerable to the issues of space-for-time substitutions (Lovell et al., 2023). These gaps and biases warrant caution when interpreting the maps and should be addressed as new datasets become available. There remain considerable potentials for future refinement and expanded applicability (Damgaard, 2019).

There are spatial gaps in the maps derived from Landsat 5 before 2013. These gaps resulted from missing observations in the Landsat 5 archive and the satellite's decommissioning in 2012. Such gaps may affect the temporal analysis, particularly in regions where data availability is temporally biased.

2.4 Inclusion of future data and modification

We encourage the incorporation of new data and methods using our framework by providing open assess to our model fitting code as an example. Although we used the random forest model, we encourage users to explore

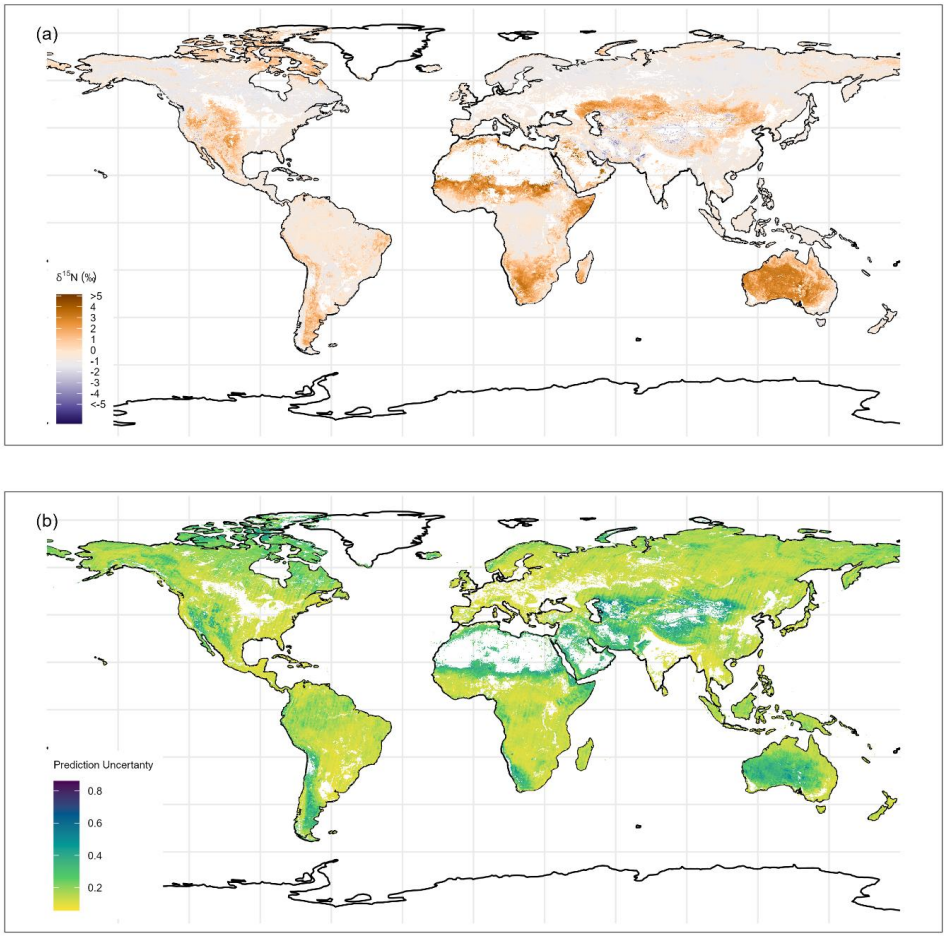
https://doi.org/10.5194/essd-2026-738
Preprint. Discussion started: 16 November 2026
© Author(s) 2026. CC BY 4.0 License.



other hyperparameters and alternative modelling approaches. GEE supports several different machine learning models (see: https://developers.google.com/earth-engine/guides/machine-learning).

3 Results

An example of $\delta^{15}N$ map in 2020 with uncertainty is shown in Fig 3. Maps from other years could be explored on GEE via the application we provided. There were large spatial variations of $\delta^{15}N$ (Fig 3a), with higher $\delta^{15}N$ values in areas with greater prediction uncertainty (Fig 3a and b). Most of the pixels (99 %) fall between -2.2 and 3.4 with a median of -0.7 in 2020 (Fig 4a). The latitudinal patterns in 1990 and 2020 showed that the change of $\delta^{15}N$ was not globally uniform, with decrease more common at northern high latitudes and increase more common in mid-latitudes (Fig 4b).



https://doi.org/10.5194/essd-2026-738
Preprint. Discussion started: 16 November 2026
© Author(s) 2026. CC BY 4.0 License.



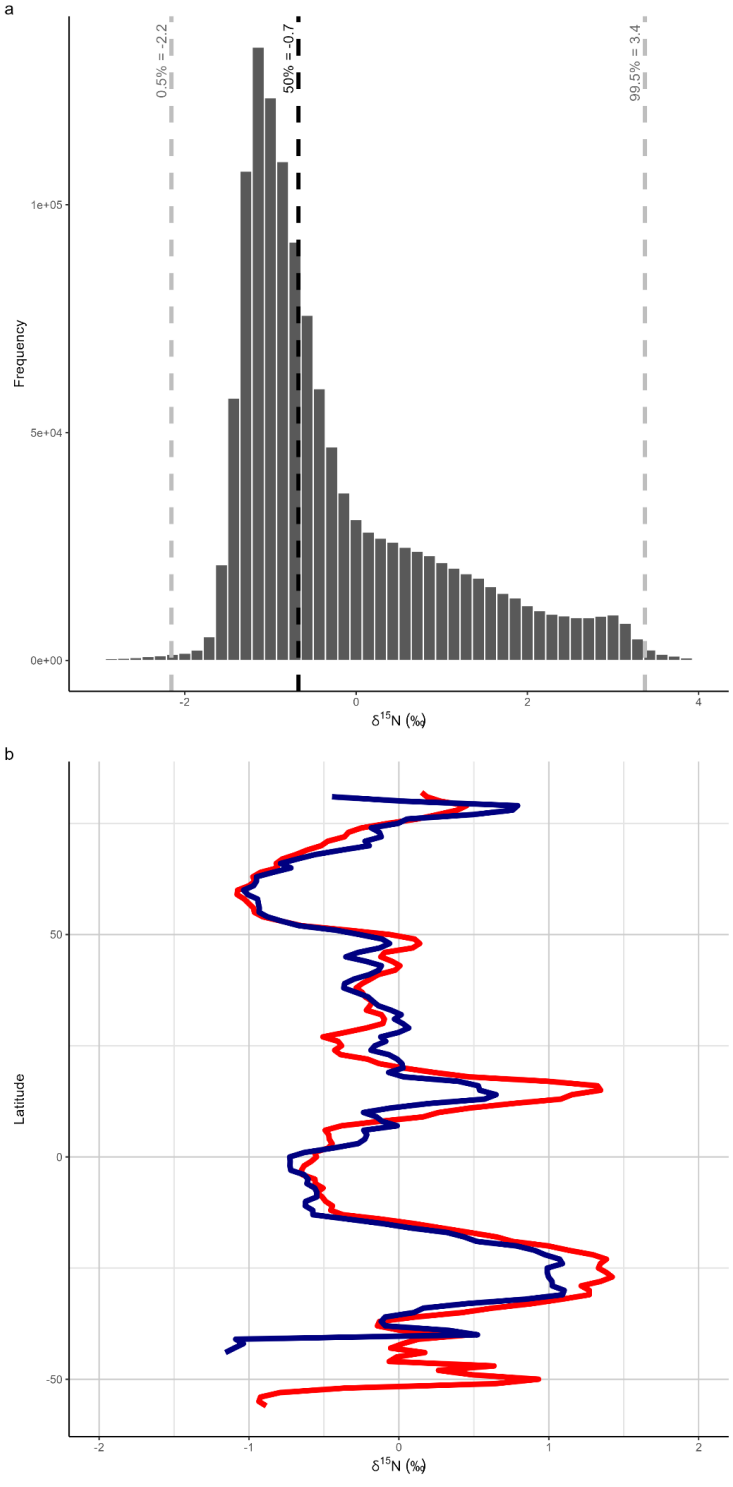
172 **Figure 3. Spatiotemporal variation of $\delta^{15}N$. (a) $\delta^{15}N$ map for 2020. The map excludes land cover types**
173 **with intense human modifications (i.e., croplands & built-up). (b) The prediction uncertainty of 2020 as**
174 **an example.**

175

https://doi.org/10.5194/essd-2026-738
Preprint. Discussion started: 16 November 2026
© Author(s) 2026. CC BY 4.0 License.



Open Access Earth System Science Data Discussions



176

https://doi.org/10.5194/essd-2026-738
Preprint. Discussion started: 16 November 2026
© Author(s) 2026. CC BY 4.0 License.



Figure 4. Frequency distribution and latitudinal patterns of foliar $\delta^{15}N$. (a) The distribution of median $\delta^{15}N$ aggregated to 10 km resolution in 2020. Vertical lines show the 0.5 %, 50 % and 99.5 % quantiles. (b) The latitudinal pattern of $\delta^{15}N$ in 1990 compared with those in 2020.

A unique feature of our maps was their high spatial resolution. We provide two examples of global biodiversity hotspots (Fig 5). In both the Cerrado, Brazil and Madagascar, pronounced environmental variation caused vegetation communities to shift drastically within small geographical distances. The $\delta^{15}N$ maps captured these fine scale differences, with areas of more sparse vegetation showing high $\delta^{15}N$ values (darker colour in Fig 5 a and d). Notably, the spatial patterns of $\delta^{15}N$ does not simply follow that of vegetation greenness (Fig 5 c and f), suggesting potential for $\delta^{15}N$ to reveal aspects of vegetation change beyond those captured by vegetation indices.

We further showed temporal change of $\delta^{15}N$ in Jingbian County, Shaanxi, China from 2000 to 2022 with reforestation in 2010 (Fig 6). Initially, $\delta^{15}N$ declined with increasing greenness; however, after 2015, when vegetation greenness saturated (Fig 6b), $\delta^{15}N$ continued to decline (Fig 6d). Example code and functions to map additional regions and years are provided here: https://code.earthengine.google.com/447b5ee8c987d54db7bf183e7224203e. In addition, time series data and maps can be accessed via the code-free app (https://tern-landscapes.earthengine.app/view/nitrogen-availability).

https://doi.org/10.5194/essd-2026-738
Preprint. Discussion started: 16 November 2026
© Author(s) 2026. CC BY 4.0 License.

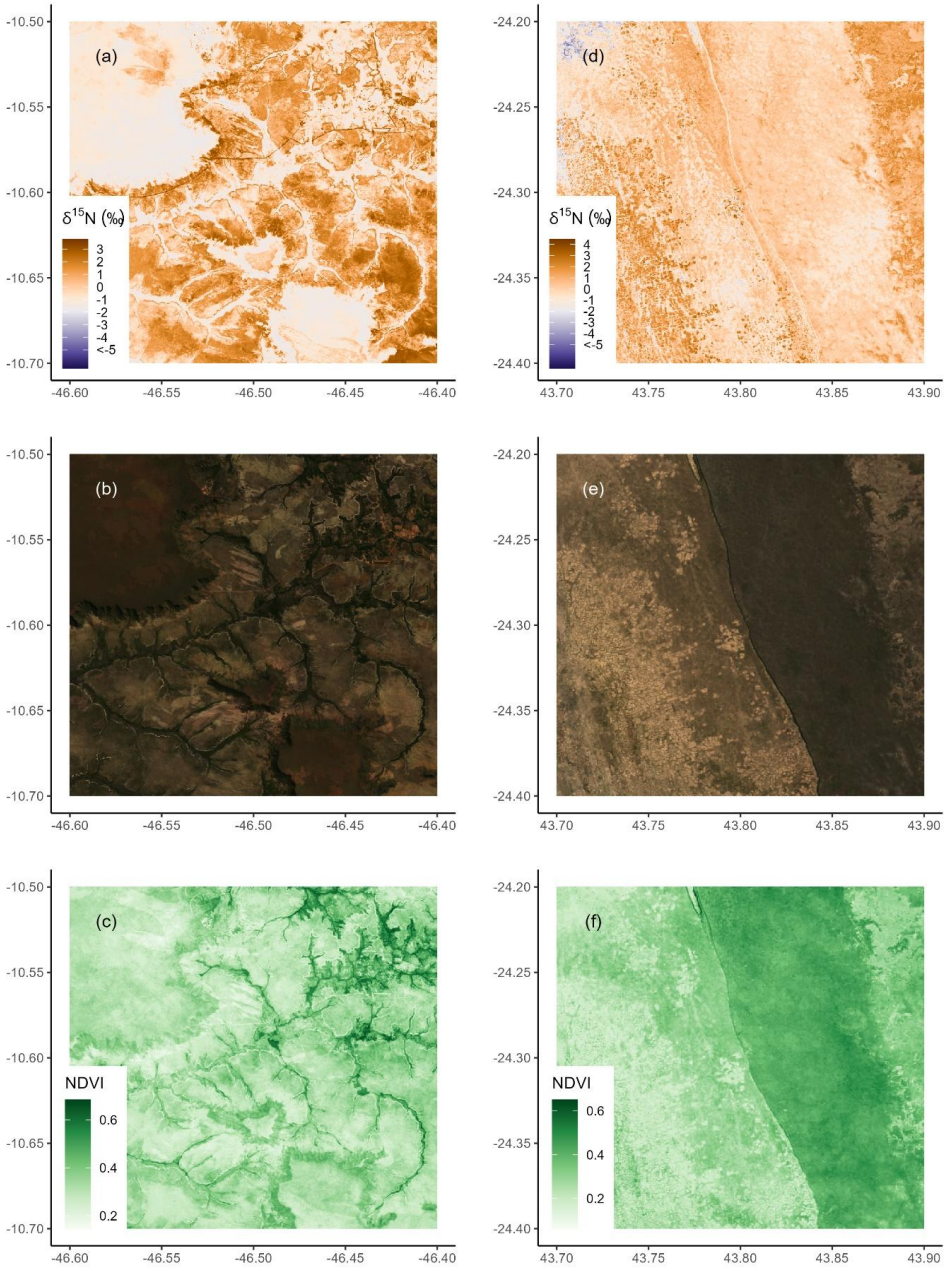
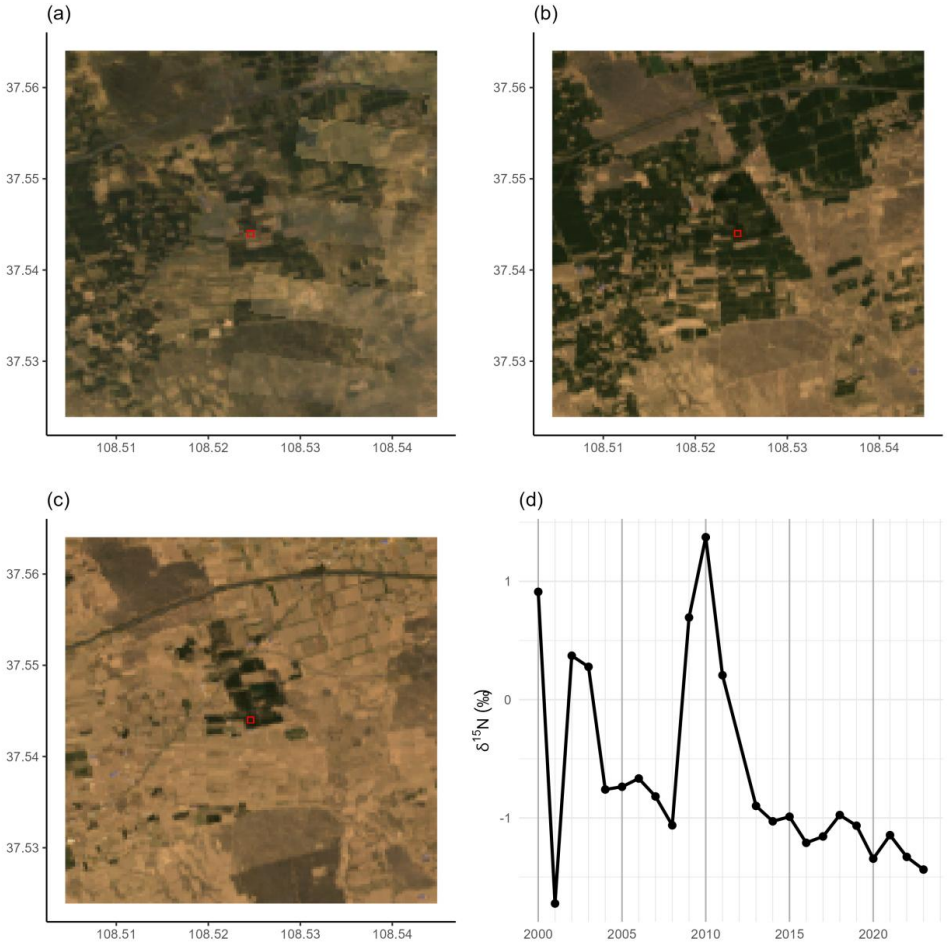


Figure 5. Examples showing $\delta^{15}N$ of 2022 of two biodiversity hotspots: Estação Ecológica Serra Geral do Tocantins, Cerrado, Brazil (a, b, c) and Tsimanampetsotse National Park, Madagascar (d, e ,f). Parts (a) and (d) show $\delta^{15}N$, (b) and (e) show the RGB image, while (c) and (f) show NDVI from Landsat of the

https://doi.org/10.5194/essd-2026-738
Preprint. Discussion started: 16 November 2026
© Author(s) 2026. CC BY 4.0 License.



199 **same region. The regions are selected based on Myers et al. (2000) and the uncertainty of the $\delta^{15}N$ maps**
200 **(Fig 3b).**



201

202 **Figure 6. Time series of $\delta^{15}N$ of a reforestation site in Jingbian County, Shaanxi, China. (a-c) show the**
203 **Landsat RGB photos of 2010, 2015, and 2020, respectively. The red squares show the reforestation site.**
204 **(d) shows the time series of $\delta^{15}N$ from 2000 with reforestation in 2010.**

205

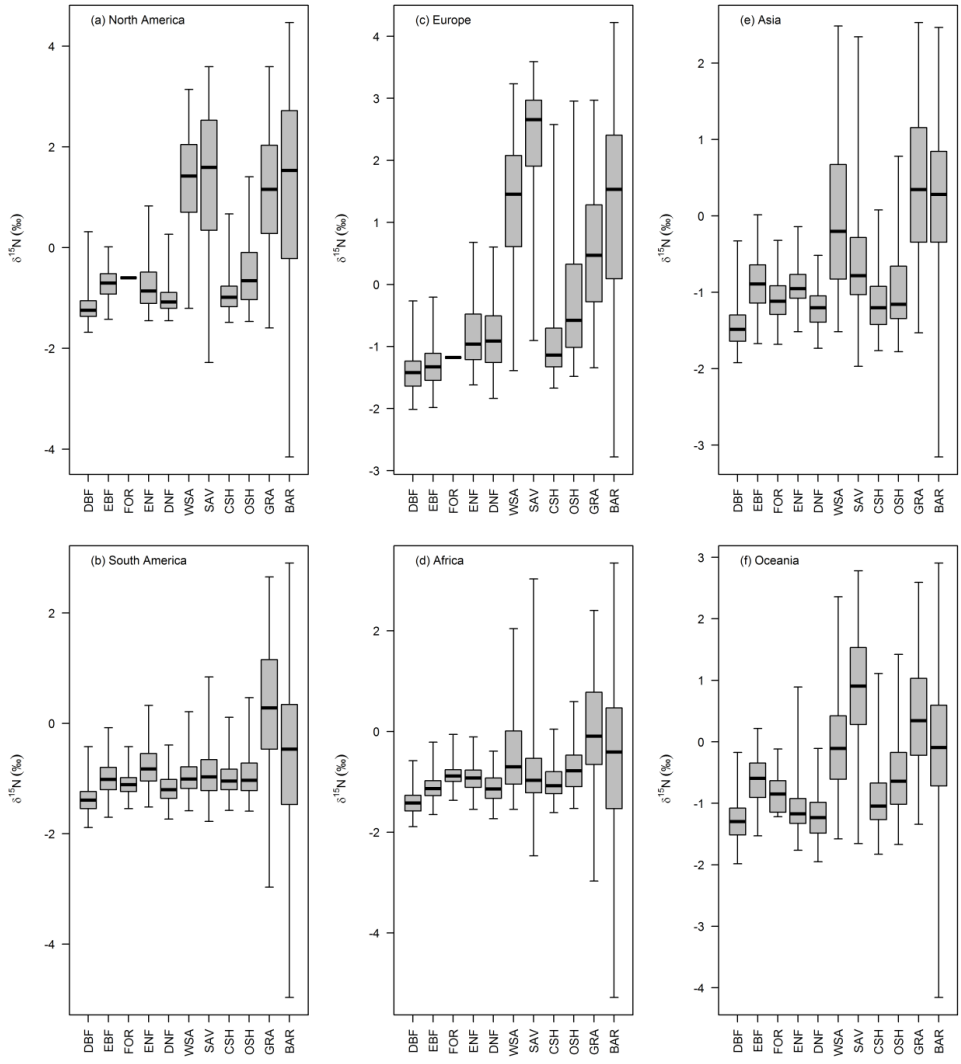
206 Gaining knowledge of how $\delta^{15}N$ is distributed over space and time is important. We report the $\delta^{15}N$ for each
207 land use type in each continent to partially account for the spatial variation (Fig 7). Across continents, land
208 cover types with higher grass cover consistently showed high $\delta^{15}N$ than other land cover types with high woody

https://doi.org/10.5194/essd-2026-738
Preprint. Discussion started: 16 November 2026
© Author(s) 2026. CC BY 4.0 License.



209 cover. Noticing this land cover dependence, we showed the temporal change of the median $\delta^{15}N$ in each year
210 over 1984-2023 (Fig 8). Except for Open and Closed Shrublands, other land cover types showed conservative
211 changes in the median with grassland showing largest increase and evergreen needle leaf forests showing the
212 largest decrease.

213



214

215 **Figure 7. Median $\delta^{15}N$ values for each land cover type in each continent averaged over 1984-2023. The**
216 **region names correspond to the grids shown in Fig 2. Keys indicate different land cover types**

https://doi.org/10.5194/essd-2026-738
Preprint. Discussion started: 16 November 2026
© Author(s) 2026. CC BY 4.0 License.



Open Access Earth System Science Data Discussions

(https://doi.org/10.5067/MODIS/MCD12C1.061): DBF - Deciduous Broadleaf Forests; EBF - Evergreen Broadleaf Forests; FOR - Mixed Forests; ENF - Evergreen Needleleaf Forests; DNF - Deciduous Needleleaf Forests; WSA - Woody Savannas; SAV - Savannas; CSH - Closed Shrublands; OSH - Open Shrublands; GRA - Grasslands; BAR - Barren.

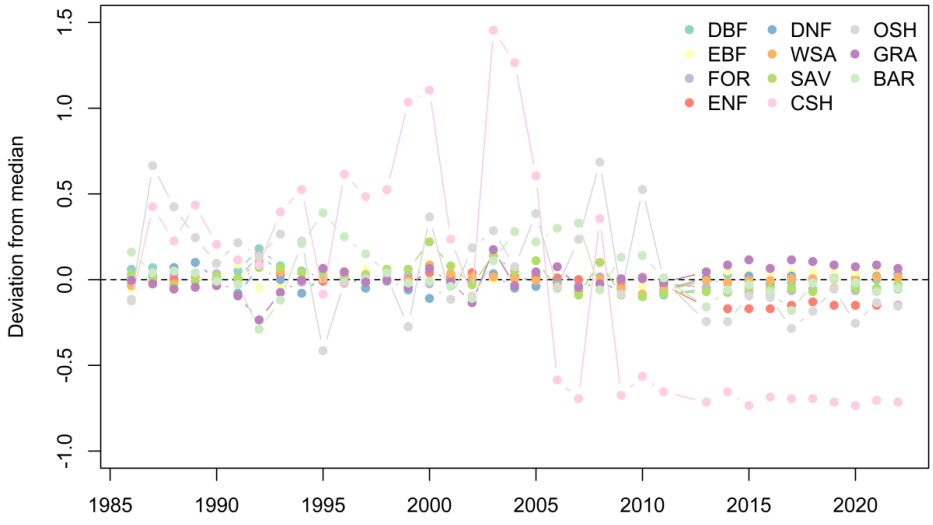
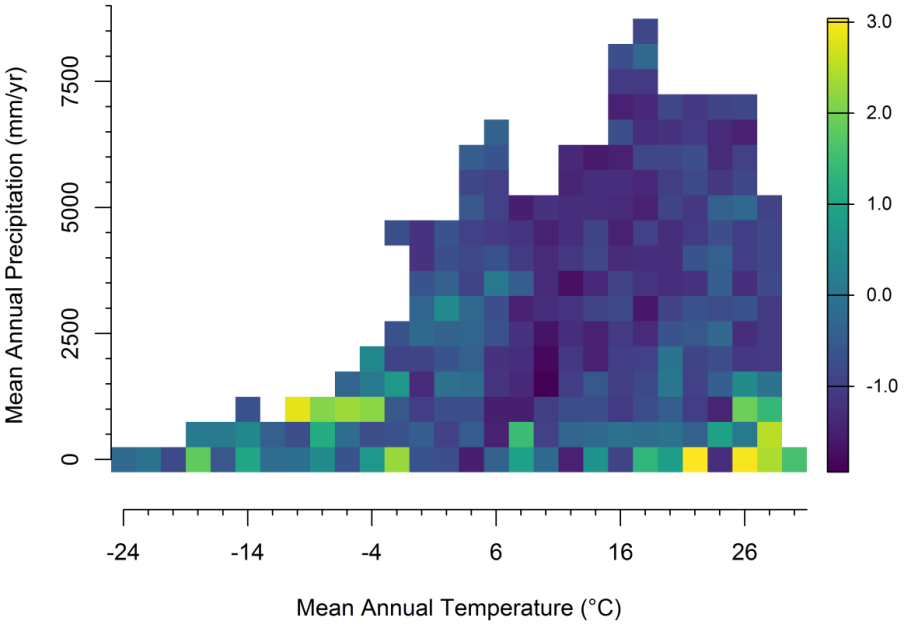


Fig 8. Change in median $\delta^{15}N$ of each land cover type over 1984-2023. The black dashed line shows the overall median of all data. There are no data in 2012 due to the decommissioning of Landsat 5. The large variation of the data is due to gaps in Landsat 5 (Fig 10). Keys are consistent with the caption of Fig 7.

The spatial continuity of the $\delta^{15}N$ maps allowed further investigation of the drivers of spatial variation. We preliminarily explored the impacts of mean annual precipitation and mean annual temperature on $\delta^{15}N$ in 2020 (Fig 9). Results indicated that high $\delta^{15}N$ values were more common in regions with low rainfall, whereas low $\delta^{15}N$ values were prevalent in temperate, high-precipitation regions.

https://doi.org/10.5194/essd-2026-738
Preprint. Discussion started: 16 November 2026
© Author(s) 2026. CC BY 4.0 License.



231

232 **Fig 9. The global $\delta^{15}N$ of 2020 distribution over the mean annual temperature (MAT) and mean annual**
233 **precipitation (MAP) gradients.**

234

235 Although our maps were spatiotemporally continuous, the number of available Landsat observations differed by
236 year (Fig 10a) and by region (Fig 10b). Overall, Landsat 5 provided less consistent spatiotemporal coverage,
237 capturing only half of the Earth surface compared to Landsat 8. As a result, maps before 2012 which rely solely
238 on Landsat 5, exhibited greater spatial gaps and were based on fewer Landsat retrievals per year. The impacts of
239 these data gaps were uneven across different land cover types (Fig 8).

240

https://doi.org/10.5194/essd-2026-738
Preprint. Discussion started: 16 November 2026
© Author(s) 2026. CC BY 4.0 License.

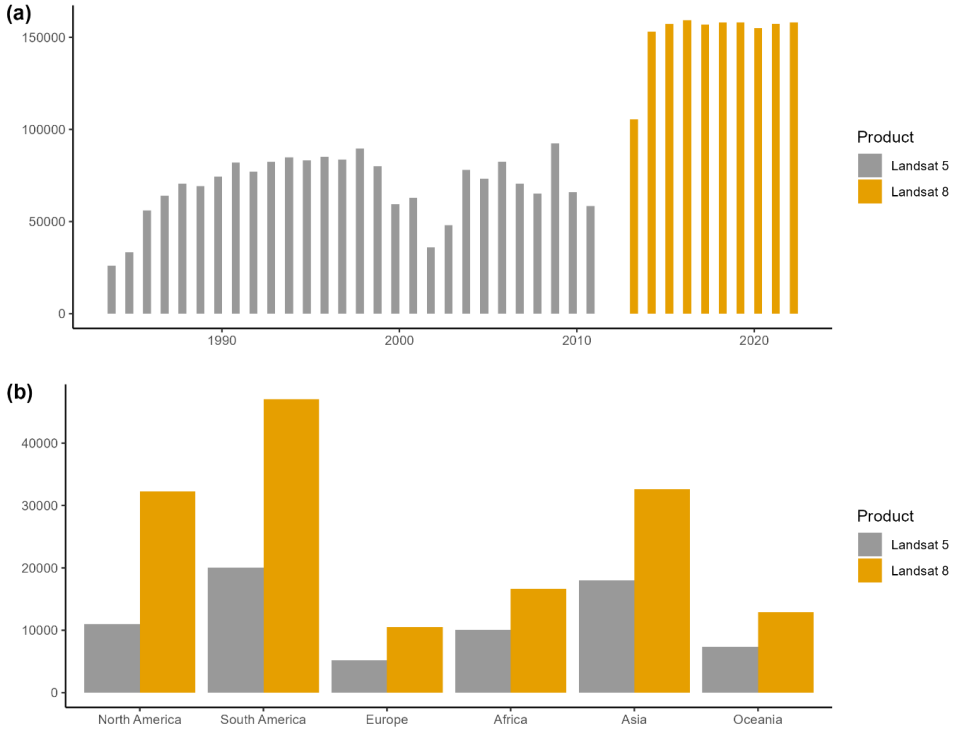


Fig 10. Global pixel numbers by year (a) and annual pixel numbers per continent (b). Region names correspond to the grid divisions shown in Fig 2.

4 Discussion

The impacts of anthropogenic environmental changes on global nitrogen cycles have been difficult to assess due to a lack of long-term global observations. The $\delta^{15}N$ maps provided here offer both the spatiotemporal resolution and global coverage needed to address critical questions in global change ecology. These maps can be integrated into process-based models to investigate the drivers underlying changes in terrestrial nitrogen cycles. Moreover, temporal trends in $\delta^{15}N$ can help identify changes in vegetation and microbial communities and thus aid monitoring of ecosystem condition changes.

4.1 Implications for nitrogen cycle modelling

https://doi.org/10.5194/essd-2026-738
Preprint. Discussion started: 16 November 2026
© Author(s) 2026. CC BY 4.0 License.



Our $\delta^{15}N$ spatiotemporal data offer the opportunity to overcome long-standing limitations in nitrogen cycle modelling. The lack of nitrogen observations at spatiotemporal resolutions comparable to land surface models has prevented robust evaluation of nitrogen process modelling and its response to anthropogenic environmental change. At site scales, widespread evidence suggests that nitrogen would be more limiting under elevated atmospheric CO_2 due to carbon enrichment (Luo et al., 2004; Reich et al., 2006; Manson et al., 2022). However, it remains unclear whether plants can accommodate or adapt to the carbon rich environment and how such responses would affect plant photosynthesis (Ainsworth and Long, 2005). Existing observations are usually based on a limited set of species or locations, often discontinuous over time, and sometimes yield contradictory results (Mason et al., 2022). The combined impacts of elevated CO_2 and other environmental factors on nitrogen cycles therefore remains to be tested, leaving the question of whether terrestrial plants will face increased nitrogen limitation unresolved at the global scale.

Long term foliar $\delta^{15}N$ observations could help detect such accommodation or adaptation processes. Model data synthesis, increasingly used to obtain parameters in process-based models (Higgins et al., 2023; Tao et al., 2024), can quantify 'response traits' —functional traits that determine how the nitrogen cycle responds to environmental variations (Lavorel and Garnier, 2002). Applying model data synthesis across space and time could provide spatiotemporal dynamics of these traits, shedding light on intra-generational (i.e., accommodation) and inter-generational (i.e., adaptation) responses to environmental changes. Such insights could enable land surface models to represent accommodation and adaptation more realistically, reducing uncertainty of future carbon and climate projections.

Previous studies reported high spatial variation in foliar $\delta^{15}N$ as well as its temporal trends (Craine et al., 2018). While some variation resulted from species turnover, the contribution of environment factors could also be important. Quantifying the impacts of each environmental variable requires analysing the $\delta^{15}N$ time series in a process-based modelling framework (Caldararu et al., 2022). The global $\delta^{15}N$ time series enables such analysis, providing the data to identify processes that driven the changes in global nitrogen cycles.

A major ongoing debate concerns whether $\delta^{15}N$ is a reliable indicator of plant nitrogen availability (Hiltbrunner et al., 2019; Tang et al., 2022). One complicating factor is separating the impacts of anthropogenic nitrogen deposition from environmental controls on plant $\delta^{15}N$. Anthropogenic nitrogen deposition is an alternative nitrogen source and may have a similar isotopic signature as the biotic nitrogen fixation (i.e., ^{15}N depleted). It is also important to answer to what degree does anthropogenic nitrogen deposition relieve the enhanced nitrogen

https://doi.org/10.5194/essd-2026-738
Preprint. Discussion started: 16 November 2026
© Author(s) 2026. CC BY 4.0 License.



demand of terrestrial plants. Together with high resolution anthropogenic nitrogen deposition maps (Tian et al., 2023), our $\delta^{15}N$ dataset facilitates integrated modelling and remote sensing approaches to partition the impacts of multiple drivers. This can help resolve the debate over when, where and how $\delta^{15}N$ can be reliably used as a proxy for plant nitrogen availability (e.g., Caldararu et al., 2022; Higgins et al., 2023).

4.2 Implications for plant trait mapping

Although future vegetation can be measured with emerging technologies, past observations provide essential knowledge for understanding on how plant communities have responded to environmental changes. Building on the multidecadal Landsat dataset, our maps provide a global view of $\delta^{15}N$ distribution and its temporal dynamics, and the framework can be applied to other plant chemical traits using emerging new multi/hyperspectral remote sensing products.

A key feature of our maps is the use of only remote sensing data (i.e., excluding any environmental covariates). We made this decision because of two reasons. First, the environmental covariates may only capture the autocorrelation and thus provide pseudo statistics (Ploton et al., 2020). Second, in theory, the vegetation chemical composition should be directly measured by reflectance, independent of the environment. Indeed, Yang et al. (2025) showed that adding long-term climate variables does not improve the model performance. Our maps relying only on remote sensing data thus allow change detection and attribution of environmental drivers of the change in $\delta^{15}N$ based on observations of the vegetation.

We also address the challenge of canopy effects—structural factors such as leaf area and angle that influence scaling from leaf to canopy reflectance—through innovative cross-validation, transforming a complex biophysical problem into a tractable statistical one. Downscaling the canopy reflectance to leaf level has been done with radiative transfer models (e.g., Cherif et al., 2023). However, applying radiative transfer models to global trait mapping bare two key challenges. First, the models require iteration to solve for parameters (i.e., traits) and thus are computationally demanding, preventing high resolution high frequency mapping. Second, the models often assume that the vegetation is homogeneous within each pixel and time period which prevents its application to dynamic ecosystems that are spatiotemporally heterogeneous (Darvishzadeh et al., 2008). However, using cross validation and all six Landsat channels, our framework statistically addressed the canopy effects. Canopy effects on vegetation reflectance apply to all six channels of Landsat but nitrogen absorbance peaks are mostly in the near infrared bands (Hellmann et al., 2015; Wang et al., 2017). This difference allows using the other bands to statistically account for canopy effect to correct the nitrogen related bands (e.g.,

https://doi.org/10.5194/essd-2026-738
Preprint. Discussion started: 16 November 2026
© Author(s) 2026. CC BY 4.0 License.



Knyazikhin et al., 2013). The cross validation on a representable training dataset should allow the random forest model to account for the canopy effect.

Although many previous trait maps provide code and data in open access repository, the accessibility of the data and code may depend on the skills of the users. This is because the complex code generally requires access to high performance computing to reproduce and deep knowledge of programming to use. Moreover, when the spatiotemporal resolution becomes finer, it becomes impractical and inefficient to download the global data to a local storage. We provide a web-based application allowing for visualisation and download of the global $\delta^{15}N$ time series at 30 m resolution with no requirement of computation and coding skills. Advanced users can take advantage of our open access code to reproduce the maps, to test alternative models, and to add new datasets with no requirement of local storage or computational resources. The various examples provided above should facilitate users with different needs to obtain the data in the format needed.

4.3 Implications for ecosystem condition monitoring

The time series of $\delta^{15}N$ provided an opportunity to monitor the compositional change in terrestrial ecosystems and thus could be used as an indicator of ecosystem condition. Global biodiversity initiatives identified three aspects of indicators for terrestrial ecosystem condition assessment: function, composition, and structure (e.g., SEEA-EA; TNFD; UN Convention on Biological Diversity; Kunming-Montréal Global Biodiversity Framework). However, nitrogen cycles, arguably one of the most important elements to creatures on Earth, have been largely ignored, due to a lack of indicators globally. $\delta^{15}N$ could provide the missing knowledge on nitrogen cycles for ecosystem condition assessment and is one of the few indicators that can be measured from leaf to canopy scales.

The $\delta^{15}N$ could be used as a proxy of plant and soil microbe composition change. Our knowledge on ecosystem compositional changes mostly relies on abundance data from a small selection of species and locations which do not capture the fine resolution changes (e.g., Dornelas et al., 2018; Bruelheide et al., 2019). Meanwhile, $\delta^{15}N$ has been shown to be sensitive to change in vegetation and soil microbe compositions (e.g., Craine et al., 2009; Hofmeister et al., 2012; Hawke, 2017; Craine et al., 2018). $\delta^{15}N$ and changes in $\delta^{15}N$ could thus be a useful indicator of compositional change in plant and soil microbes. Moreover, our $\delta^{15}N$ maps as well as previous studies highlight the potential to combine plant traits and vegetation reflectance to investigate biodiversity changes (e.g., Bush et al, 2017; Ma et al., 2019; Zheng et al., 2021), reemphasising the key role of plant traits in

https://doi.org/10.5194/essd-2026-738
Preprint. Discussion started: 16 November 2026
© Author(s) 2026. CC BY 4.0 License.



biodiversity monitoring (Furey and Tilman, 2023). The spatiotemporal coverage of satellite derived trait maps thus provided a unique prospect on global vegetation and could facilitate biodiversity monitoring.

Nitrogen is an important element of fertilisers, supporting growing human food demand (Foley et al., 2011) but also a threat to terrestrial and aquatic ecosystem biodiversity (Zhang et al., 2015). Although our $\delta^{15}N$ spatiotemporal data do not cover cropland, the method we developed could be applied to monitor fertilisation intensity and potentially help optimise the use of fertiliser (Cai et al., 2023). Moreover, the $\delta^{15}N$ can be predicted at high temporal resolution with hyperspectral measurements (e.g., near-field or drone-based remote sensing), providing a near-real time measure of terrestrial nitrogen processes. The high resolution $\delta^{15}N$ could thus be used in an ecological forecasting framework to inform farm and water quality management (e.g., Carey et al., 2021).

Code and data availability

The spatiotemporal data are publicly available via DOI: https://doi.org/10.25919/zxvv-bj04 (Yang et al., 2026). The code to generate the spatiotemporal data are available on Google Earth Engine: https://code.earthengine.google.com/b291ce3e6131a5f0aa121a796143d43a.

To encourage use of the spatiotemporal data for researchers with limited coding skills and/or no access to could computing, we visualised the spatiotemporal data with a web-app that requires no coding and registration to access, please see: https://tern-landscapes.earthengine.app/view/nitrogen-availability

Author Contributions

J.Y. and H.Z. conceived the study. J.V. and T.R.M. developed large scale mapping and online application. H.Z. obtained the ground-based observations and developed the reflectance method. Y.G. obtained the Landsat data. J.Y. obtained gridded environmental data and developed the random forest fitting. J.Y. performed the analysis and wrote the initial manuscript. R.P., Y.F. and K.M, and P.R. provided critical comments on the manuscript. T.R.M., K.M. and S.K. acquired the funding. All authors contributed to interpreting the results and editing the paper.

Acknowledgement

This research was partly funded by Terrestrial Ecosystem Research Network (TERN), an Australian Government National Collaborative Research Infrastructure Strategy (NCRIS) enabled project and used TERN infrastructure.

https://doi.org/10.5194/essd-2026-738
Preprint. Discussion started: 16 November 2026
© Author(s) 2026. CC BY 4.0 License.



References

Ainsworth, E. A. and Long, S. P.: What have we learned from 15 years of free-air CO_2 enrichment (FACE)? A meta-analytic review of the responses of photosynthesis, canopy properties and plant production to rising CO_2, New Phytologist, 165, 351–372, https://doi.org/10.1111/j.1469-8137.2004.01224.x, 2004.

BassiriRad, H., Constable, J. V. H., Lussenhop, J., Kimball, B. A., Norby, R. J., Oechel, W. C., Reich, P. B., Schlesinger, W. H., Zitzer, S., Sehtiya, H. L., and Silim, S.: Widespread foliage $\delta^{15}N$ depletion under elevated CO_2: inferences for the nitrogen cycle, Global Change Biology, 9, 1582–1590, https://doi.org/10.1046/j.1365-2486.2003.00679.x, 2003.

Bowman, D. M. J. S., Kolden, C. A., Abatzoglou, J. T., Johnston, F. H., van der Werf, G. R., and Flannigan, M.: Vegetation fires in the Anthropocene, Nature Reviews Earth and Environment, 1, 500–515, https://doi.org/10.1038/s43017-020-0085-3, 2020.

Brookshire, E. N. J., Stoy, P. C., Currey, B., and Finney, B.: The greening of the Northern Great Plains and its biogeochemical precursors, Global Change Biology, 26, 5404–5413, https://doi.org/10.1111/gcb.15115, 2020.

Bruelheide, H., Dengler, J., Jiménez-Alfaro, B., Purschke, O., Hennekens, S. M., Chytrý, M., Pillar, V. D., Jansen, F., Kattge, J., Sandel, B., Aubin, I., Biurrun, I., Field, R., Haider, S., Jandt, U., Lenoir, J., Peet, R. K., Peyre, G., Sabatini, F. M., Schmidt, M., Schrodt, F., Winter, M., Aćić, S., Agrillo, E., Alvarez, M., Ambarlı, D., Angelini, P., Apostolova, I., Arfin Khan, M. A. S., Arnst, E., Attorre, F., Baraloto, C., Beckmann, M., Berg, C., Bergeron, Y., Bergmeier, E., Bjorkman, A. D., Bondareva, V., Borchardt, P., Botta-Dukát, Z., Boyle, B., Breen, A., Brisse, H., Byun, C., Cabido, M. R., Casella, L., Cayuela, L., Černý, T., Chepinoga, V., Csiky, J., Curran, M., Ćušterevska, R., Dajić Stevanović, Z., De Bie, E., de Ruffray, P., De Sanctis, M., Dimopoulos, P., Dressler, S., Ejrnæs, R., El-Sheikh, M. A. E. M., Enquist, B., Ewald, J., Fagúndez, J., Finckh, M., Font, X., Forey, E., Fotiadis, G., García-Mijangos, I., Gasper, A. L., Golub, V., Gutierrez, A. G., Hatim, M. Z., He, T., Higuchi, P., Holubová, D., Hölzel, N., Homeier, J., Indreica, A., Işık Gürsoy, D., Jansen, S., Janssen, J., Jedrzejek, B., Jiroušek, M., Jürgens, N., Kącki, Z., Kavgacı, A., Kearsley, E., Kessler, M., Knollová, I., Kolomiychuk, V., Korolyuk, A., Kozhevnikova, M., Kozub, Ł., Krstonošić, D., Kühl, H., Kühn, I., Kuzemko, A., Küzmič, F., Landucci, F., et al.: sPlot – A new tool for global vegetation analyses, Journal of Vegetation Science, 30, 161–186, https://doi.org/10.1111/jvs.12710, 2019.

Bush, A., Sollmann, R., Wilting, A., Bohmann, K., Cole, B., Balzter, H., Martius, C., Zlinszky, A., Calvignac-Spencer, S., Cobbold, C. A., Dawson, T. P., Emerson, B. C., Ferrier, S., Gilbert, M. T. P., Herold, M., Jones, L.,

https://doi.org/10.5194/essd-2026-738
Preprint. Discussion started: 16 November 2026
© Author(s) 2026. CC BY 4.0 License.

Leendertz, F. H., Matthews, L., Millington, J. D. A., Olson, J. R., Ovaskainen, O., Raffaelli, D., Reeve, R., Rödel, M.-O., Rodgers, T. W., Snape, S., Visseren-Hamakers, I., Vogler, A. P., White, P. C. L., Wooster, M. J., and Yu, D. W.: Connecting Earth observation to high-throughput biodiversity data, Nat Ecology and Evolution, 1, 0176, https://doi.org/10.1038/s41559-017-0176, 2017.

Cai, S., Zhao, X., Pittelkow, C. M., Fan, M., Zhang, X., and Yan, X.: Optimal nitrogen rate strategy for sustainable rice production in China, Nature, 615, 73–79, https://doi.org/10.1038/s41586-022-05678-x, 2023.

Caldararu, S., Thum, T., Yu, L., Kern, M., Nair, R., and Zaehle, S.: Long-term ecosystem nitrogen limitation from foliar $\delta^{15}N$ data and a land surface model, Global Change Biology, 28, 493–508, https://doi.org/10.1111/gcb.15933, 2022.

Carey, C., Woelmer, W., Lofton, M., Figueiredo, R. J., Bookout, B., Corrigan, R., Daneshmand, V., Hounshell, A., Howard, D. W., Lewis, A. S. L., McClure, R., Wander, H., Ward, N., and Thomas, R. Q.: Advancing lake and reservoir water quality management with near-term, iterative ecological forecasting, Inland Waters, 12, 107–120, https://doi.org/10.1080/20442041.2020.1816421, 2021.

Cherif, E., Feilhauer, H., Berger, K., Dao, P. D., Ewald, M., Hank, T. B., He, Y., Kovach, K. R., Lu, B., Townsend, P. A., and Kattenborn, T.: From spectra to plant functional traits: Transferable multi-trait models from heterogeneous and sparse data, Remote Sensing of Environment, 292, 113580, https://doi.org/10.1016/j.rse.2023.113580, 2023.

Craine, J. M., Elmore, A. J., Aidar, M. P. M., Bustamante, M., Dawson, T. E., Hobbie, E. A., Kahmen, A., Mack, M. C., McLauchlan, K. K., Michelsen, A., Nardoto, G. B., Pardo, L. H., Peñuelas, J., Reich, P. B., Schuur, E. A. G., Stock, W. D., Templer, P. H., Virginia, R. A., Welker, J. M., and Wright, I. J.: Global patterns of foliar nitrogen isotopes and their relationships with climate, mycorrhizal fungi, foliar nutrient concentrations, and nitrogen availability, New Phytologist, 183, 980–992, https://doi.org/10.1111/j.1469-8137.2009.02917.x, 2009.

Craine, J. M., Elmore, A. J., Wang, L., Aranibar, J., Bauters, M., Boeckx, P., Crowley, B. E., Dawes, M. A., Delzon, S., Fajardo, A., Fang, Y., Fujiyoshi, L., Gray, A., Guerrieri, R., Gundale, M. J., Hawke, D. J., Hietz, P., Jonard, M., Kearsley, E., Kenzo, T., Makarov, M., Marañón-Jiménez, S., McGlynn, T. P., McNeil, B. E., Mosher, S. G., Nelson, D. M., Peri, P. L., Roggy, J. C., Sanders-DeMott, R., Song, M., Szpak, P., Templer, P. H., Van der Colff, D., Werner, C., Xu, X., Yang, Y., Yu, G., and Zmudczyńska-Skarbek, K.: Isotopic evidence

https://doi.org/10.5194/essd-2026-738
Preprint. Discussion started: 16 November 2026
© Author(s) 2026. CC BY 4.0 License.



425 for oligotrophication of terrestrial ecosystems, Nature Ecology and Evolution, 2, 1735–1744,
426 https://doi.org/10.1038/s41559-018-0694-0, 2018.

427 Damgaard, C.: A Critique of the Space-for-Time Substitution Practice in Community Ecology, Trends in
428 Ecology & Evolution, 34, 416–421, https://doi.org/10.1016/j.tree.2019.01.013, 2019.

429 Darvishzadeh, R., Skidmore, A., Schlerf, M., and Atzberger, C.: Inversion of a radiative transfer model for
430 estimating vegetation LAI and chlorophyll in a heterogeneous grassland, Remote Sensing of Environment, 112,
431 2592–2604, https://doi.org/10.1016/j.rse.2007.12.003, 2008.

432 Dornelas, M., Antão, L. H., Moyes, F., Bates, A. E., Magurran, A. E., Adam, D., Akhmetzhanova, A. A.,
433 Appeltans, W., Arcos, J. M., Arnold, H., Ayyappan, N., Badihi, G., Baird, A. H., Barbosa, M., Barreto, T. E.,
434 Bässler, C., Bellgrove, A., Belmaker, J., Benedetti-Cecchi, L., Bett, B. J., Bjorkman, A. D., Błażewicz, M.,
435 Blowes, S. A., Bloch, C. P., Bonebrake, T. C., Boyd, S., Bradford, M., Brooks, A. J., Brown, J. H., Bruelheide,
436 H., Budy, P., Carvalho, F., Castañeda-Moya, E., Chen, C. A., Chamblee, J. F., Chase, T. J., Siegwart Collier, L.,
437 Collinge, S. K., Condit, R., Cooper, E. J., Cornelissen, J. H. C., Cotano, U., Kyle Crow, S., Damasceno, G.,
438 Davies, C. H., Davis, R. A., Day, F. P., Degraer, S., Doherty, T. S., Dunn, T. E., Durigan, G., Duffy, J. E.,
439 Edelist, D., Edgar, G. J., Elahi, R., Elmendorf, S. C., Enemar, A., Ernest, S. K. M., Escribano, R., Estiarte, M.,
440 Evans, B. S., Fan, T., Turini Farah, F., Loureiro Fernandes, L., Farneda, F. Z., Fidelis, A., Fitt, R., Fosaa, A. M.,
441 Daher Correa Franco, G. A., Frank, G. E., Fraser, W. R., García, H., Cazzolla Gatti, R., Givan, O.,
442 Gorgone-Barbosa, E., Gould, W. A., Gries, C., Grossman, G. D., Gutierréz, J. R., Hale, S., Harmon, M. E.,
443 Harte, J., Haskins, G., Henshaw, D. L., Hermanutz, L., Hidalgo, P., Higuchi, P., Hoey, A., Van Hoey, G.,
444 Hofgaard, A., Holeck, K., Hollister, R. D., Holmes, R., Hoogenboom, M., Hsieh, C., Hubbell, S. P., Huettmann,
445 F., Huffard, C. L., Hurlbert, A. H., et al.: BioTIME: A database of biodiversity time series for the Anthropocene,
446 Global Ecology Biogeography, 27, 760–786, https://doi.org/10.1111/geb.12729, 2018.

447 Foley, J. A., Ramankutty, N., Brauman, K. A., Cassidy, E. S., Gerber, J. S., Johnston, M., Mueller, N. D.,
448 O'Connell, C., Ray, D. K., West, P. C., Balzer, C., Bennett, E. M., Carpenter, S. R., Hill, J., Monfreda, C.,
449 Polasky, S., Rockström, J., Sheehan, J., Siebert, S., Tilman, D., and Zaks, D. P. M.: Solutions for a cultivated
450 planet, Nature, 478, 337–342, https://doi.org/10.1038/nature10452, 2011.

451 Furey, G. N. and Tilman, D.: Plant chemical traits define functional and phylogenetic axes of plant biodiversity,
452 Ecology Letters, 26, 1394–1406, https://doi.org/10.1111/ele.14262, 2023.

https://doi.org/10.5194/essd-2026-738
Preprint. Discussion started: 16 November 2026
© Author(s) 2026. CC BY 4.0 License.



453 Galloway, J. N., Townsend, A. R., Erisman, J. W., Bekunda, M., Cai, Z., Freney, J. R., Martinelli, L. A.,
454 Seitzinger, S. P., and Sutton, M. A.: Transformation of the Nitrogen cycle: Recent Trends, Questions, and
455 Potential Solutions, Science, 320, 889–892, https://doi.org/10.1126/science.1136674, 2008.

456 Garten, C. T., Iversen, C. M., and Norby, R. J.: Litterfall ^{15} N abundance indicates declining soil nitrogen
457 availability in a free-air CO_2 enrichment experiment, Ecology, 92, 133–139, https://doi.org/10.1890/10-0293.1,
458 2011.

459 Hawke, D.: Foliar and soil N and δ15N as restoration metrics at Pūtaringamotu Riccarton Bush, Christchurch
460 city, Journal of the Royal Society of New Zealand, 47, https://doi.org/10.1080/03036758.2017.1281319, 2017.

461 Hellmann, C., Große-Stoltenberg, A., Lauströ, V., Oldeland, J., and Werner, C.: Retrieving nitrogen isotopic
462 signatures from fresh leaf reflectance spectra: disentangling δ15N from biochemical and structural leaf
463 properties, Frontiers of Plant Sciience, 6, https://doi.org/10.3389/fpls.2015.00307, 2015.

464 Hietz, P., Turner, B. L., Wanek, W., Richter, A., Nock, C. A., and Wright, S. J.: Long-term Change in the
465 Nitrogen Cycle of Tropical Forests, Science, 334, 664–666, https://doi.org/10.1126/science.1211979, 2011.

466 Higgins, S. I., Conradi, T., and Muhoko, E.: Shifts in vegetation activity of terrestrial ecosystems attributable to
467 climate trends, Nature Geoscience, 16, 147–153, https://doi.org/10.1038/s41561-022-01114-x, 2023.

468 Hiltbrunner, E., Körner, C., Meier, R., Braun, S., and Kahmen, A.: Data do not support large-scale
469 oligotrophication of terrestrial ecosystems, Nat Ecology and Evolution, 3, 1285–1286,
470 https://doi.org/10.1038/s41559-019-0948-5, 2019.

471 Hofmeister, J., Hosek, J., Buzek, F., and Rolecek, J.: Foliar N concentration and δ15N signature reflect the herb
472 layer species diversity and composition in oak-dominated forests, Applied Vegetation Science, 15,
473 https://doi.org/10.1111/j.1654-109X.2011.01174.x, 2012.

474 Hungate, B. A., Dukes, J. S., Shaw, M. R., Luo, Y., and Field, C. B.: Nitrogen and Climate Change, Science,
475 302, 1512–1513, https://doi.org/10.1126/science.1091390, 2003.

476 Jacquemoud, S., Verhoef, W., Baret, F., Bacour, C., Zarco-Tejada, P. J., Asner, G. P., François, C., and Ustin, S.
477 L.: PROSPECT+SAIL models: A review of use for vegetation characterization, Remote Sensing of
478 Environment, 113, S56–S66, https://doi.org/10.1016/j.rse.2008.01.026, 2009.

https://doi.org/10.5194/essd-2026-738
Preprint. Discussion started: 16 November 2026
© Author(s) 2026. CC BY 4.0 License.



Jansson, J. K. and Hofmockel, K. S.: Soil microbiomes and climate change, Nat Review Microbiology, 18, 35–46, https://doi.org/10.1038/s41579-019-0265-7, 2020.

Jarvis, A., H.I. Reuter, A. Nelson, E. Guevara. 2008. Hole-filled SRTM for the globe Version 4, available from the CGIAR-CSI SRTM 90m Database: https://srtm.csi.cgiar.org.

Jaureguiberry, P., Titeux, N., Wiemers, M., Bowler, D. E., Coscieme, L., Golden, A. S., Guerra, C. A., Jacob, U., Takahashi, Y., Settele, J., Díaz, S., Molnár, Z., and Purvis, A.: The direct drivers of recent global anthropogenic biodiversity loss, Science Advances, 8, eabm9982, https://doi.org/10.1126/sciadv.abm9982, 2022.

Knyazikhin, Y., Schull, M. A., Stenberg, P., Mõttus, M., Rautiainen, M., Yang, Y., Marshak, A., Latorre Carmona, P., Kaufmann, R. K., Lewis, P., Disney, M. I., Vanderbilt, V., Davis, A. B., Baret, F., Jacquemoud, S., Lyapustin, A., and Myneni, R. B.: Hyperspectral remote sensing of foliar nitrogen content, Proceeding of National Academy of Sciences U.S.A., 110, https://doi.org/10.1073/pnas.1210196109, 2013.

Kou, D., Yang, G., Li, F., Feng, X., Zhang, D., Mao, C., Zhang, Q., Peng, Y., Ji, C., Zhu, Q., Fang, Y., Liu, X., Xu-Ri, Li, S., Deng, J., Zheng, X., Fang, J., and Yang, Y.: Progressive nitrogen limitation across the Tibetan alpine permafrost region, Nature Communications, 11, 3331, https://doi.org/10.1038/s41467-020-17169-6, 2020.

Lavorel, S. and Garnier, E.: Predicting changes in community composition and ecosystem functioning from plant traits: revisiting the Holy Grail, Functional Ecology, 16, 545–556, https://doi.org/10.1046/j.1365-2435.2002.00664.x, 2002.

Li, H.: Smile, 2014. https://haifengl.github.io

Luo, Y., Su, B., Currie, W. S., Dukes, J. S., Finzi, A., Hartwig, U., Hungate, B., McMurtrie, R. E., Oren, R., Parton, W. J., Pataki, D. E., Shaw, M. R., Zak, D. R., and Field, C. B.: Progressive Nitrogen Limitation of Ecosystem Responses to Rising Atmospheric Carbon Dioxide, BioScience, 54, 731, https://doi.org/10.1641/0006-3568(2004)054[0731:PNLOER]2.0.CO;2, 2004.

Ma, X., Mahecha, M. D., Migliavacca, M., van der Plas, F., Benavides, R., Ratcliffe, S., Kattge, J., Richter, R., Musavi, T., Baeten, L., Barnoaiea, I., Bohn, F. J., Bouriaud, O., Bussotti, F., Coppi, A., Domisch, T., Huth, A., Jaroszewicz, B., Joswig, J., Pabon-Moreno, D. E., Papale, D., Selvi, F., Laurin, G. V., Valladares, F.,

https://doi.org/10.5194/essd-2026-738
Preprint. Discussion started: 16 November 2026
© Author(s) 2026. CC BY 4.0 License.



506 Reichstein, M., and Wirth, C.: Inferring plant functional diversity from space: the potential of Sentinel-2,
507 Remote Sensing of Environment, 233, 111368, https://doi.org/10.1016/j.rse.2019.111368, 2019.

508 Mason, R. E., Craine, J. M., Lany, N. K., Jonard, M., Ollinger, S. V., Groffman, P. M., Fulweiler, R. W.,
509 Angerer, J., Read, Q. D., Reich, P. B., Templer, P. H., and Elmore, A. J.: Evidence, causes, and consequences of
510 declining nitrogen availability in terrestrial ecosystems, Science, 376, eabh3767,
511 https://doi.org/10.1126/science.abh3767, 2022.

512 McLauchlan, K. K., Ferguson, C. J., Wilson, I. E., Ocheltree, T. W., and Craine, J. M.: Thirteen decades of
513 foliar isotopes indicate declining nitrogen availability in central North American grasslands, New Phytologist,
514 187, 1135–1145, https://doi.org/10.1111/j.1469-8137.2010.03322.x, 2010.

515 Montandon, L. and Small, E.: The impact of soil reflectance on the quantification of the green vegetation
516 fraction from NDVI, Remote Sensing of Environment, 112, 1835–1845,
517 https://doi.org/10.1016/j.rse.2007.09.007, 2008.

518 Ploton, P., Mortier, F., Réjou-Méchain, M., Barbier, N., Picard, N., Rossi, V., Dormann, C., Cornu, G.,
519 Viennois, G., Bayol, N., Lyapustin, A., Gourlet-Fleury, S., and Pélissier, R.: Spatial validation reveals poor
520 predictive performance of large-scale ecological mapping models, Nauret Communications, 11, 4540,
521 https://doi.org/10.1038/s41467-020-18321-y, 2020.

522 Polley, H. W., Derner, J. D., Jackson, R. B., Gill, R. A., Procter, A. C., and Fay, P. A.: Plant community change
523 mediates the response of foliar δ15N to CO_2 enrichment in mesic grasslands, Oecologia, 178, 591–601,
524 https://doi.org/10.1007/s00442-015-3221-x, 2015.

525 Reich, P. B., Hobbie, S. E., Lee, T., Ellsworth, D. S., West, J. B., Tilman, D., Knops, J. M. H., Naeem, S., and
526 Trost, J.: Nitrogen limitation constrains sustainability of ecosystem response to CO_2, Nature, 440, 922–925,
527 https://doi.org/10.1038/nature04486, 2006.

528 Reich, P. B., Tjoelker, M. G., Pregitzer, K. S., Wright, I. J., Oleksyn, J., and Machado, J. L.: Scaling of
529 respiration to nitrogen in leaves, stems and roots of higher land plants, Ecology Letters, 11, 793–801,
530 https://doi.org/10.1111/j.1461-0248.2008.01185.x, 2008.

531 Reich, P.B., Mohanbabu, N., Isbell, F., Hobbie, S.E., Butler, E.E., 2024. High CO_2 dampens then amplifies N-
532 induced diversity loss over 24 years. Nature 635, 370–375. https://doi.org/10.1038/s41586-024-08066-9

https://doi.org/10.5194/essd-2026-738
Preprint. Discussion started: 16 November 2026
© Author(s) 2026. CC BY 4.0 License.



Robinson, D.: δ15N as an integrator of the nitrogen cycle, Trends in Ecology & Evolution, 16, 153–162, https://doi.org/10.1016/S0169-5347(00)02098-X, 2001.

Roy, D. P., Kovalskyy, V., Zhang, H. K., Vermote, E. F., Yan, L., Kumar, S. S., and Egorov, A.: Characterization of Landsat-7 to Landsat-8 reflective wavelength and normalized difference vegetation index continuity, Remote Sensing of Environment, 185, 57–70, https://doi.org/10.1016/j.rse.2015.12.024, 2016.

Ruehr, S., Keenan, T. F., Williams, C., Zhou, Y., Lu, X., Bastos, A., Canadell, J. G., Prentice, I. C., Sitch, S., and Terrer, C.: Evidence and attribution of the enhanced land carbon sink, Nat Review Earth Environmont, 4, 518–534, https://doi.org/10.1038/s43017-023-00456-3, 2023.

Serbin, S. P., Singh, A., McNeil, B. E., Kingdon, C. C., and Townsend, P. A.: Spectroscopic determination of leaf morphological and biochemical traits for northern temperate and boreal tree species, Ecological Applications, 24, 1651–1669, https://doi.org/10.1890/13-2110.1, 2014.

Tang, S., Liu, J., Gilliam, F. S., Hietz, P., Wang, Z., Lu, X., Zeng, F., Wen, D., Hou, E., Lai, Y., Fang, Y., Tu, Y., Xi, D., Huang, Z., Zhang, D., Wang, R., and Kuang, Y.: Drivers of foliar ^{15}N trends in southern China over the last century, Global Change Biology, 28, 5441–5452, https://doi.org/10.1111/gcb.16285, 2022.

Tao, F., Houlton, B. Z., Huang, Y., Wang, Y., Manzoni, S., Ahrens, B., Mishra, U., Jiang, L., Huang, X., and Luo, Y.: Convergence in simulating global soil organic carbon by structurally different models after data assimilation, Global Change Biology, 30, e17297, https://doi.org/10.1111/gcb.17297, 2024.

Tian, H., Bian, Z., Shi, H., Qin, X., Pan, N., Lu, C., Pan, S., Tubiello, F. N., Chang, J., Conchedda, G., Liu, J., Mueller, N., Nishina, K., Xu, R., Yang, J., You, L., and Zhang, B.: History of anthropogenic Nitrogen inputs (HaNi) to the terrestrial biosphere: a 5 arcmin resolution annual dataset from 1860 to 2019, Earth System Science Data, 14, 4551–4568, https://doi.org/10.5194/essd-14-4551-2022, 2022.

Walker, A. P., De Kauwe, M. G., Bastos, A., Belmecheri, S., Georgiou, K., Keeling, R. F., McMahon, S. M., Medlyn, B. E., Moore, D. J. P., Norby, R. J., Zaehle, S., Anderson-Teixeira, K. J., Battipaglia, G., Brienen, R. J. W., Cabugao, K. G., Cailleret, M., Campbell, E., Canadell, J. G., Ciais, P., Craig, M. E., Ellsworth, D. S., Farquhar, G. D., Fatichi, S., Fisher, J. B., Frank, D. C., Graven, H., Gu, L., Haverd, V., Heilman, K., Heimann, M., Hungate, B. A., Iversen, C. M., Joos, F., Jiang, M., Keenan, T. F., Knauer, J., Körner, C., Leshyk, V. O., Leuzinger, S., Liu, Y., MacBean, N., Malhi, Y., McVicar, T. R., Penuelas, J., Pongratz, J., Powell, A. S., Riutta, T., Sabot, M. E. B., Schleucher, J., Sitch, S., Smith, W. K., Sulman, B., Taylor, B., Terrer, C., Torn, M. S.,

https://doi.org/10.5194/essd-2026-738
Preprint. Discussion started: 16 November 2026
© Author(s) 2026. CC BY 4.0 License.



561 Treseder, K. K., Trugman, A. T., Trumbore, S. E., Van Mantgem, P. J., Voelker, S. L., Whelan, M. E., and
562 Zuidema, P. A.: Integrating the evidence for a terrestrial carbon sink caused by increasing atmospheric CO_2,
563 New Phytologist, 229, 2413–2445, https://doi.org/10.1111/nph.16866, 2021.

564 Wang, L., Okin, G. S., Wang, J., Epstein, H., and Macko, S. A.: Predicting leaf and canopy ^{15}N compositions
565 from reflectance spectra, Geophysical Research Letters, 34, L02401, https://doi.org/10.1029/2006GL028506,
566 2007.

567 Wang, Y., Niu, G., Wang, R., Rousk, K., Li, A., Hasi, M., Wang, C., Xue, J., Yang, G., Lü, X., Jiang, Y., Han,
568 X., and Huang, J.: Enhanced foliar ^{15}N enrichment with increasing nitrogen addition rates: Role of plant species
569 and nitrogen compounds, Global Change Biology,16555, https://doi.org/10.1111/gcb.16555, 2022.

570 Wang, Z., Skidmore, A. K., Wang, T., Darvishzadeh, R., Heiden, U., Heurich, M., Latifi, H., and Hearne, J.:
571 Canopy foliar nitrogen retrieved from airborne hyperspectral imagery by correcting for canopy structure effects,
572 International Journal of Applied Earth Observation and Geoinformation, 54, 84–94,
573 https://doi.org/10.1016/j.jag.2016.09.008, 2017.

574 Yang, J., Zhang, H., Guo, Y., Donohue, R.J., McVicar, T.R., Ferrier, S., Müller, W., Lü, X., Fang, Y., Wang,
575 X., Reich, P.B., Han, X., Mokany, K., 2025. Globally Mapping the Nitrogen Stable Isotope Ratios of Terrestrial
576 Vegetation From 1984 to 2022. Earth's Future, 13, e2024EF005836. https://doi.org/10.1029/2024EF005836

577 Yang, Jinyan; Pasut, Chiara; Pagendam, Dan; Ugbaje, Sebastian; & Karunaratne, Senani (2026): Steady-state
578 soil organic carbon and fractionation for Australian cropland. v2. CSIRO. Data Collection.
579 https://doi.org/10.25919/zxvv-bj04

580 Zhang, X., Davidson, E. A., Mauzerall, D. L., Searchinger, T. D., Dumas, P., and Shen, Y.: Managing nitrogen
581 for sustainable development, Nature, 528, 51–59, https://doi.org/10.1038/nature15743, 2015.

582 Zheng, Z., Zeng, Y., Schneider, F., Zhao, Y., Zhao, D., Schmid, B., Schaepman, M., and Morsdorf, F.: Mapping
583 functional diversity using individual tree-based morphological and physiological traits in a subtropical forest,
584 Remote Sensing of Environment, https://doi.org/10.1016/j.rse.2020.112170, 2021.

585 Zhu, Z., Piao, S., Myneni, R. B., Huang, M., Zeng, Z., Canadell, J. G., Ciais, P., Sitch, S., Friedlingstein, P.,
586 Arneth, A., Cao, C., Cheng, L., Kato, E., Koven, C., Li, Y., Lian, X., Liu, Y., Liu, R., Mao, J., Pan, Y., Peng, S.,
587 Peñuelas, J., Poulter, B., Pugh, T. A. M., Stocker, B. D., Viovy, N., Wang, X., Wang, Y., Xiao, Z., Yang, H.,

https://doi.org/10.5194/essd-2026-738
Preprint. Discussion started: 16 November 2026
© Author(s) 2026. CC BY 4.0 License.



588 Zaehle, S., and Zeng, N.: Greening of the Earth and its drivers, Nature Climate Change, 1–6,
589 https://doi.org/10.1038/nclimate3004, 2016.